An LDA-Based Approach for Real-Time Simultaneous Classification of Movements Using Surface Electromyography

Chris Wilson Antuvan, *Student Member, IEEE*, and Lorenzo Masia, *Member, IEEE*

***Abstract*— Myoelectric-based decoding strategies offer significant advantages in the areas of human-machine interactions because they are intuitive and require less cognitive effort from the users. However, a general drawback in using machine learning techniques for classification is that the decoder is limited to predicting only one movement at any instant and hence restricted to performing the motion in a sequential manner, whereas human motor control strategy involves simultaneous actuation of multiple degrees of freedom (DOFs) and is considered to be a natural and efficient way of performing tasks. Simultaneous decoding in the context of myoelectric-based movement control is a challenge that is being addressed recently and is increasingly popular. In this paper, we propose a novel classification strategy capable of decoding both the individual and combined movements, by collecting data from only the individual motions. Additionally, we exploit low-dimensional representation of the myoelectric signals using a supervised decomposition algorithm called linear discriminant analysis, to simplify the complexity of control and reduce computational cost. The performance of the decoding algorithm is tested in an online context for the two DOFs task comprising the hand and wrist movements. Results indicate an overall classification accuracy of 88.02% for both the individual and combined motions.**

***Index Terms*— Electromyography, simultaneous motion decoding, real-time myoelectric control, linear discriminant analysis.**

I. Introduction

MYOELECTRICALLY controlled prosthesis and exoskeletons devices aim at closely replicating the natural and efficient motor control strategies of the human [1]–[3]. The intention decoding becomes challenging in joints with multiple DOFs (especially distal joints such as wrist and hand which are capable of highly dexterous manipulation), where a single muscle could be responsible for more than one movement [4]. Therefore, decoding user intention can be challenging due to the complex relationship between the muscle activity and the corresponding motions [5]. Furthermore, using surface electromyographic (sEMG) techniques makes it harder to access the activity of the deeper muscle fibers, avoid cross-talk in the signals, and are very sensitive to sweat, fatigue and slight shift in electrode positions [6]. For this reason, pattern recognition techniques using machine learning algorithms have primarily been used in decoding myoelectric signals corresponding to various movements or gestures, and are capable of providing reliable classification accuracies [7], [8]. These strategies proposed a decoder which can only predict one movement or gesture at a time, lacking the capability to simultaneously classify multiple movements when the user voluntarily performs a combined motion. To overcome this limitation, muscle activities of both the individual and combined movements are also recorded during the calibration phase in order to enhance the capability of the decoder to perform simultaneous classification [9]. Young *et al.* [10] proposed a modified version for simultaneous classification, to enhance the reliability of decoding, but their approach in general is limited by the need for an extensive calibration process which is time consuming.

Various linear and non-linear regression-based algorithms have been proposed for performing simultaneous and proportional decoding of multiple DOFs using surface electromyography [11]–[19]. Most of these techniques require a calibration phase where the muscle activities of only the individual movements are recorded; a regression-based algorithm is used to build the relationship between the muscle activity and the desired output (position or force) for each DOF separately and are then combined in order to predict both individual and combined movements. The decoding strategy proposed by Jiang *et al.* [16] is a widely used method for performing proportional and simultaneous decoding, and involves using non-negative matrix factorization (NMF) to reduce the dimensionality and build the control scheme for each individual DOF.

Alternatively, an approach called linear enhanced training has been proposed by Nowak *et al.* [20], where the authors built a relationship for the combined movements as a function of the muscle activity of the respective individual movements. The approach required to record the sEMG signals of both individual and combined movements from a small subset of subjects initially, in order to build the relationship.

Manuscript received April 23, 2018; revised July 24, 2018 and September 12, 2018; accepted September 27, 2018. Date of publication February 22, 2019; date of current version March 22, 2019. This work was supported by the Rehabilitation Research Institute of Singapore under Grant M4062142. *(Corresponding author: Chris Wilson Antuvan.)*

C. W. Antuvan is with the School of Mechanical and Aerospace Engineering, Nanyang Technological University, Singapore 639798 (e-mail: chriswil001@e.ntu.edu.sg).

L. Masia is with the Department of Biomechanical Engineering, University of Twente, 7500 AE Enschede, The Netherlands, and also with the Institut für Technische Informatik, Heidelberg University, 69120 Heidelberg, Germany.

This paper has supplementary downloadable material available at http://ieeexplore.ieee.org, provided by the author.

Digital Object Identifier 10.1109/TNSRE.2018.2873839

In this paper, we propose a novel classification algorithm capable of predicting both individual and combined movements by recording, during the calibration phase, the surface EMG of only the individual motions. The decoding strategy is designed based on the hypothesis that the features of the combined movement data can be obtained by a combination of the data from the respective individual movement [21]. The objective of this study is to test the decoding paradigm in a task involving two DOFs of the wrist and hand movements, and evaluate its performance for real-time classification. Another aspect we are interested in exploring, is the use of dimensionality reduction techniques for simplifying control complexity and lowering the computational costs. This could be very beneficial while using an embedded system to enable portability of the processing unit in applications such as prosthesis and exoskeletons. In this case, we are interested in applying the linear discriminant analysis (LDA) method to project the EMG data to a low-dimensional space, mainly because of the supervised nature of the algorithm, by assigning labels to each movement-class to ensure better discrimination [22]. The alternative approaches for data compression, i.e. NMF and PCA aim at maximizing the variance among the data irrespective of the various movement-classes.

II. Methods

A. Decoding Model Algorithm

On a low-dimensional representation of the muscular activity, we speculate that the feature vectors of the combined movement lie in the geometrical space enclosed between those of the respective individual movements. The choice of the order of the reduced dimension using LDA is a critical factor in determining the complexity of the algorithm. In case of a two DOF motion-task (two individual movements per DOF), the simplest and least complicated choice, in terms of complexity of algorithm and computational power is a two-dimensional space.

Our proposed strategy involves projecting the original data into a two-dimensional space, where each data point is characterized by a magnitude and an orientation, like in a polar coordinate system. The orientation space for each individual movement-class is defined by an angular boundary (circular sector) which is determined based on the mean and standard deviation of the orientation of the data in each class. More specifically, if the data lies within the two boundaries then it is classified as belonging to that respective movement-class. Whereas, if the data lies outside the boundaries it is classified as a combined movement corresponding to the combination of the individual classes adjacent to it on either side. An ideal representation of the proposed decoding strategy is shown in Figure 1. The shaded area in grey represents the data space of the various individual movements of the two DOFs. The area enclosed between the individual classes are the respective combined movements.

However, the validity of this decoding model is dependent on two important criteria:

1) *Orientation constraint:* Data of one agonist/antagonistic DOF pair lies in between the data of the other pair in the orientation space. The decoder loses the ability to predict combined movements in the event when the agonist/antagonistic DOF pair are adjacent to each other.
2) *Linear combination:* The combined movement data lies in the orientation space enclosed by the respective individual movement-classes. This criterion is built on the validity of the first one, which means a violation of the former affects the validity of the latter but not vice versa.

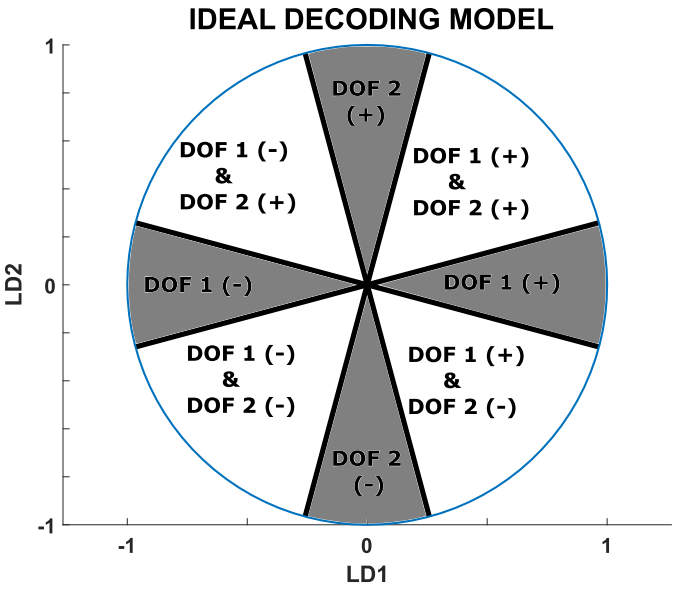

Fig. 1. Decoding model: The two DOF movements (both directions) are enclosed in the shaded region, and the respective combined movements are enclosed in the space between the individual movements.

The most important aspect to consider is that the LDA algorithm doesn't impose the *orientation constraint* criterion, which is crucial for the validation of the proposed decoding strategy. Hence, one solution that we propose is to initially project the original data to a three-dimensional space instead of two-dimensional space using LDA. It is worth noting that the two-dimensional projection of the data using LDA, is the same as projecting the three-dimensional LDA transformed data on the x-y plane. Therefore, instead of performing the default projection (on the x-y plane), we propose to identify an alternate projection of the three-dimensional data which would ensure the validity of the *orientation constraint* criterion.

The original data consisting of individual movements is represented as $X \epsilon \mathbb{R}^{m \times 4N_s}$, where m denotes the number of EMG channels, N_s is the total number of samples in each movement-class, and 4 being the number of individual classes. LDA projects the matrix X into a new matrix $\overline{X}$ given by the relation

$$\overline{X} = AX \tag{1}$$

where $A \epsilon \mathbb{R}^{3 \times m}$ is the transformation matrix which projects the data X from an m-dimensional space to a three-dimensional space, and $\overline{X} \epsilon \mathbb{R}^{3 \times 4N_s}$.

The next step is to identify an optimum rotation matrix which will ensure that the two-dimensional projection will

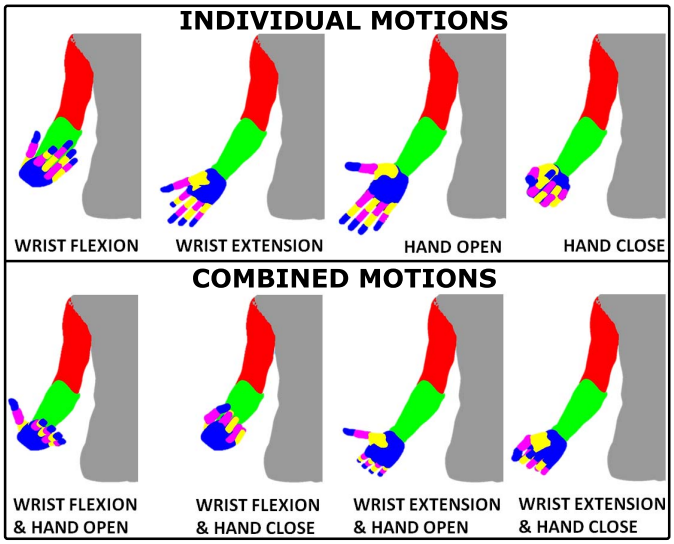

Fig. 2. Target configurations that the virtual avatar is designed to configure into, depending on the decoder output.

meet the *orientation constraint* criterion. The XYX Euler angles convention is used to obtain the rotation matrix (rotation about x axis followed by rotation about y axis, and finally rotation about x axis). The rotation matrix is given by

$$\widetilde{X}^{ijk} = \left(R3_x^k \times R2_y^j \times R1_x^i\right) \times \overline{X} \quad i, j, k \epsilon [0, 5, 10 \ldots 180] \tag{2}$$

where $R1_x^i$ is the rotation about x axis by i degrees, $R2_y^j$ is the rotation about y axis by j degrees, $R3_x^k$ is the rotation about x axis by k degrees, and $\widetilde{X}^{ijk} \epsilon \mathbb{R}^{3\times 4N_s}$.

A cost value is defined to evaluate and identify the optimal rotation matrix which will ensure the least overlap between the data of the various movement-classes, and an even distribution of data in the orientation space of the two-dimensional polar plot. The $Var_{between}^{ijk}$ measure is used to identify the projection which will ensure maximum separation between the data clusters of each movement-class. On the other hand, the Var_{within}^{ijk} measure is used to identify the best projection with minimum deviation of data within each movement-class in the orientation space. The cost value for the two-dimensional projection of $\widetilde{X}^{ijk}$ which is $\widehat{X}^{ijk} \epsilon \mathbb{R}^{2\times 4N_s}$ is evaluated only if the *orientation constraint* criterion is satisfied. The variance measures are calculated as shown in the equations below,

$$Var_{between}^{ijk} = \sum_{p=1}^{M} \frac{abs\left(\sigma^{p-} - \sigma^{p+}\right)}{\left(\sigma^{p-} + \sigma^{p+}\right)}$$

$$\sigma^{p-} = \sqrt{\frac{1}{N_s}\sum_{q=1}^{N_s}\left(\mu_p - \theta_q^{p-}\right)^2}$$

$$\sigma^{p+} = \sqrt{\frac{1}{N_s}\sum_{q=1}^{N_s}\left(\mu_p - \theta_q^{p+}\right)^2} \tag{3}$$

$$Var_{within}^{ijk} = \sum_{p=1}^{M}\sqrt{\frac{1}{N_s}\sum_{q=1}^{N_s}\left(\mu_p - \theta_q^{p}\right)^2} \tag{4}$$

where, $M = 4$ denotes the number of individual movement-classes, $p+$ and $p-$ represents the adjacent classes, on either side of the individual movement-class p, and μ and σ represent the mean and standard deviation of the orientation θ of the data points in each class p. Each of the variance measures is normalized using the z-score so as to have a common scale for computing the cost value, and the configuration $R3_x^k \times R2_y^j \times R1_x^i$ with the minimum cost value is selected as the optimal rotation matrix.

Once the optimal rotation matrix is determined, the two-dimensional projection of the data (LDA projection followed by optimal rotation) will ensure the validity of the *orientation constraint* criterion in the best possible way. The separation boundaries are fixed to twenty degrees on either side of the mean orientation of the data in each individual movement-class to have an almost even distribution of sectors for both the individual (40 degrees) and combined (50 degrees) movement-classes in the orientation space. However, the validity of the *linear combination* criterion can only be evaluated during the actual testing phase for real-time control.

B. Subjects

A total of twelve healthy subjects (eight males and four females, mean age $\pm$SD $= 27.67 \pm 1.43$ years) participated in the experiment. They all provided written informed consents prior to the commencement of the experiment. The procedures were approved by the Institutional Review Board at Nanyang Technological University.

C. Experimental Setup

The muscle activities of the subjects were recorded using a wireless EMG system (Trigno wireless, Delsys Inc.), and were acquired using a real-time data acquisition board (Quanser QPIDe), controlled in Simulink (Mathworks). The acquisition frequency was set at 1 kHz, and the output of the decoder during real-time control was averaged using a 10-sample moving window. A total of six electrodes were evenly placed around the thickest part of the forearm where most of the wrist and hand muscles are concentrated. A virtual avatar consisting of the wrist and hand articulations was displayed on a screen to provide visual feedback to the user in real-time, and the different configurations for the various individual and combined motions of the avatar are as shown in Figure 2. The myoelectric signals are pre-processed before the analysis in order to remove noise and baseline shifts. The signals are first full-wave rectified and passed to a low-pass filter (second order Butterworth filter with a cut-off frequency of 8 Hz) to obtain a linear envelope of the signal. The signal offset is removed by subtracting the mean value of each EMG channel during the rest phase.

D. Experimental Protocol

The experiments were split into two phases:

1) Calibration Phase: During this phase, a GUI instructs the subjects to perform each of the individual movements, as shown in Figure 3. Each motion is performed four times, with three seconds of motion followed by two seconds of rest,

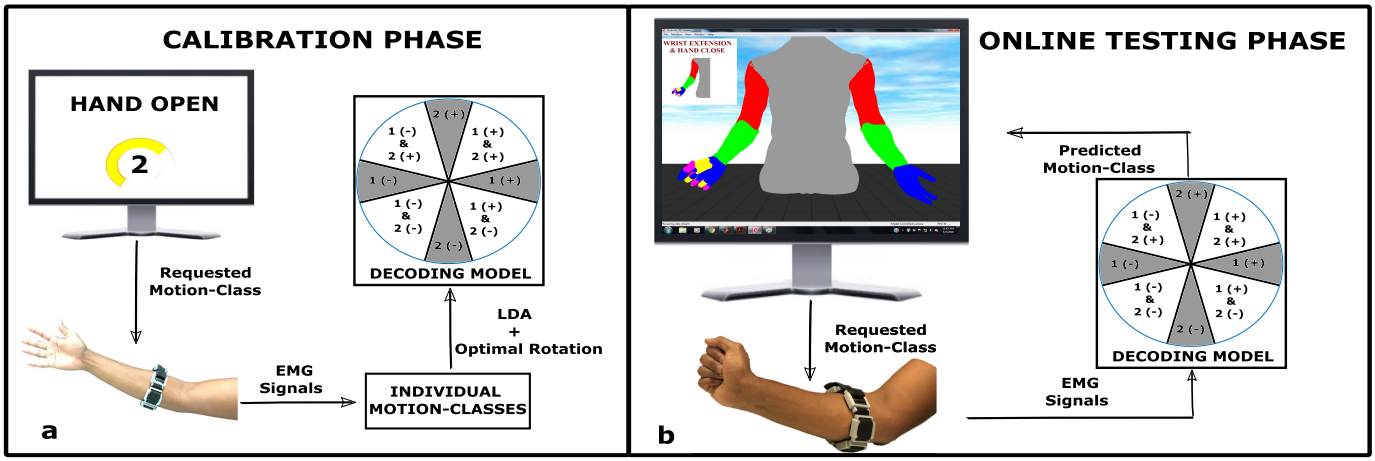

Fig. 3. Decoding model testing phase A) Calibration phase: Each user is instructed to perform a movement 4 times (alternating between three seconds of movement and two seconds of rest). A timer is shown on the screen to provide feedback. B) Online testing phase: The task to be performed is presented on the screen, and the movement performed by the user is decoded in real-time to control the motion of the virtual avatar. Visual feedback of the decoding is constantly provided, and auditory cues are provided upon successful task completion.

and the data acquired during this phase is used to build the subject-specific decoding model.

2) Online Testing Phase: The performance of the decoder is tested for real-time control in this phase. The output of the decoder is translated on the screen as a movement of the avatar, as depicted in Figure 3. The avatar is initially in a neutral position when the subject starts the experiment. The aim of the subject is to transition the avatar from the neutral pose to the target configuration of the requested movement, which is displayed on the top-left corner of the screen. The task is considered successful, only upon reaching the target position for the requested movement and holding the pose for 0.2 seconds. A minimum jerk trajectory [23] is used to control the position of the avatar; the trajectory planning algorithm produces smooth motion profiles from one configuration to another, similar to the strategy used by humans in moving the limbs, thereby ensuring a natural motion of the avatar as much as possible. The user is required to constantly produce the target motion-class in order to reach the target configuration, while the avatar returns to the neutral configuration when the user does not activate his/her muscles. It should be noted that it is not possible to start with one individual motion followed by switching to perform the other respective motion-class to complete the combined movement task. Though, it is possible to initiate the combined movement with an individual motion, the subjects still need to simultaneously produce both the requested movements at some point to reach the target and complete the task, and is generally referred to as sequential decoding. The online decoding experiments were split in two blocks to prevent muscle fatigue to the users, where each block consists of ten repetitions of each of the eight movements, performed in a pseudo-random order. The task is considered incomplete if the desired movement of the avatar is not performed within twenty seconds, after which a new task begins.

E. Intrinsic Dimensionality Estimation

One matter of concern in decoding simultaneous motions is the inadvertent activation of a combined movement when the subject only intends to perform an individual movement, leading to higher risk of task failure [24]. Therefore, it is very important to first determine whether the user is intending to perform an individual movement or a combined movement to improve the robustness and reliability of the decoder. Once it is determined, the decoding strategy can be streamlined to classify either individual or combined movements. This strategy has already been introduced in the work by Amsuess *et al.* [24], and is referred to as intrinsic dimensionality estimation (IDE).

In this work, we utilize the Mahalanobis distance (MD) measure on the LDA transformed data in order to determine whether the data belongs to an individual movement or a combined movement. The MD measure has shown to be computationally efficient and perform better compared to other IDE algorithms [24]. In this case, the MD algorithm is performed on the three-dimensional LDA transformed data consisting of only the individual movements obtained during the *calibration phase*. The MD algorithm generates a distance measure for a feature vector data with respect to a group of feature vector data (data belonging to a movement class). In general, the MD measure is calculated as shown below:

$$d_{MD} = (x - \mu)^T \Sigma^{-1} (x - \mu) \tag{5}$$

where x represents the feature vector, μ and Σ are the mean and the covariance matrix of the data belonging to the group. The mean and standard deviation of the MD measure for each of the feature vector data in a particular movement class with respect to the entire data in the same movement class is calculated as shown below in order to identify the threshold for discrimination.

$$\mu^i_{MD} = \sum_{j=1}^{N_s} (x^i_j - \mu^i)^T \Sigma_i^{-1} (x^i_j - \mu^i)$$
$$\sigma^i_{MD} = \sum_{j=1}^{N_s} (x_j - \mu^i_{MD})^2 \tag{6}$$

where μ^i_{MD} and σ^i_{MD} are the mean and standard deviation values for each movement class, x^i_j is the j^{th} feature vector

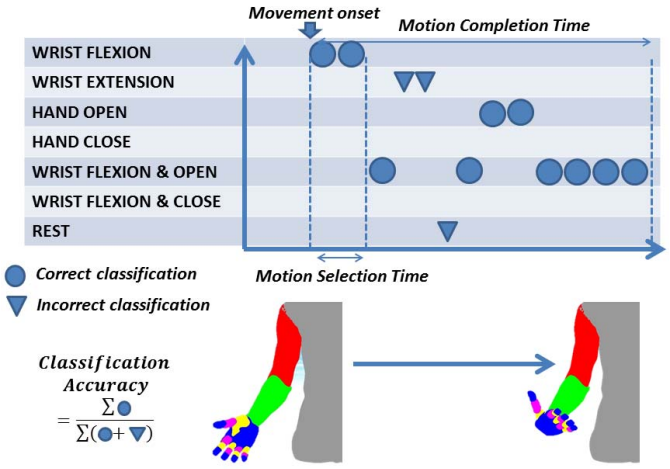

Fig. 4. Metrics used for performance evaluation, explained using an example of wrist flexion and hand open motion.

data in the i^{th} movement class, and μ^i and Σ^i are the mean and covariance matrix of the feature vector data in the i^{th} movement class. During the *online testing phase*, the MD measure is evaluated on the three-dimensional LDA transformed feature vector with respect to each of the individual movement feature data cluster (recorded during the *calibration phase*) to determine if the measure lies within the threshold for the respective movement class. The threshold is set to the mean value plus two standard deviations for each movement class.

F. Performance Metrics

We use four measures (three of them are derived from Li *et al.* [25]) to quantify the performance of the decoding model for online classification are as follows.

1) *Motion selection time:* It is the time taken by the decoder to accurately predict the desired motion-class, i.e. the time from when the subject transitions from the rest state (movement onset) to the first instant the decoder predicts the requested movement-class. The user is requested to relax to ensure that the decoder is outputting the rest state before they start performing the task. In the case of combined movements, it is calculated as the time from the onset of the first detection of movement to when the decoder accurately predicts the simultaneous movement.
2) *Motion completion time:* It is the time taken to complete the requested task, and is calculated from movement onset(as shown in Figure 4) to when the virtual avatar reaches the target configuration for the requested motion-class. Successful completion of the task is guaranteed only upon reaching the desired configuration pose and maintaining the configuration for 0.2 seconds.
3) *Online classification accuracy:* The accuracy in decoding for each successfully completed movement task is represented by this metric. In the case of combined movements, the accuracy is calculated by including the accuracy of simultaneously predicting the movement, and the accuracy of predicting the respective individual movements. This is done so as to accommodate both sequential and simultaneous decoding in the case of combined movements. The accuracy is evaluated as the ratio of the number of correctly classified samples to the total number of samples in a particular motion trial.

$$Accuracy = \frac{1}{N_t}\sum_{i=1}^{N_t}\frac{u_i}{u_i + v_i} \tag{7}$$

where N_t represents the number of successfully completed trials in a particular motion-class for a subject. u_i and v_i represents the number of correctly and incorrectly classified samples respectively in a particular trial i. Figure 4 represents the above three performance metric using an example of wrist extension motion-class.
4) *Efficiency coefficient:* This is defined as the ratio between the shortest (optimal) time required to complete the task and the actual time taken to complete the task, and expressed as a percentage. This metric is similar to the one used in [16], where instead they are calculated in terms of the optimal distance from the initial to the target. It is especially useful in the case of a combined movement task, to understand the efficiency of the user in simultaneously producing both the respective individual motions.

Statistical analysis using a student t-test at the 5% significance level is performed in order to evaluate the difference in the performance measures between individual and combined movement classes.

III. Results

The data obtained during the *calibration phase* for a representative subject is shown in Figure 5. The LDA transformation in the three-dimensional space is shown in plot A. Plot B indicates the pure two-dimensional LDA projection (projection of the three-dimensional data obtained after LDA transform on the x-y plane without performing optimal rotation), whereas plot C indicates the representation involving both LDA projection and optimal rotation. Both these projections (plot A and B) facilitates in the discrimination of the individual motions, but only the latter projection (plot B) can ensure the validity of the *orientation constraint* criteria. Therefore, the LDA plus optimal rotation transform helps in ensuring the validity of the *orientation constraint* criterion in the best possible way.

Figure 6 shows the EMG data projected on a two-dimensional space of a representative subject, during the *online testing phase*. The plot on the left indicates the data from the twenty trials for each of the individual movement-classes, whereas the plot on the right are those belonging to the combined movement-classes. It can be noticed that the data from the combined classes do indeed lie in the orientation space between the respective individual class data, thereby validating the *linear combination* criterion. Therefore, the LDA projection followed by the optimal rotation ensures the validity of both the *orientation constraint* and *linear combination* criteria, thereby enabling the working of our proposed decoding strategy.

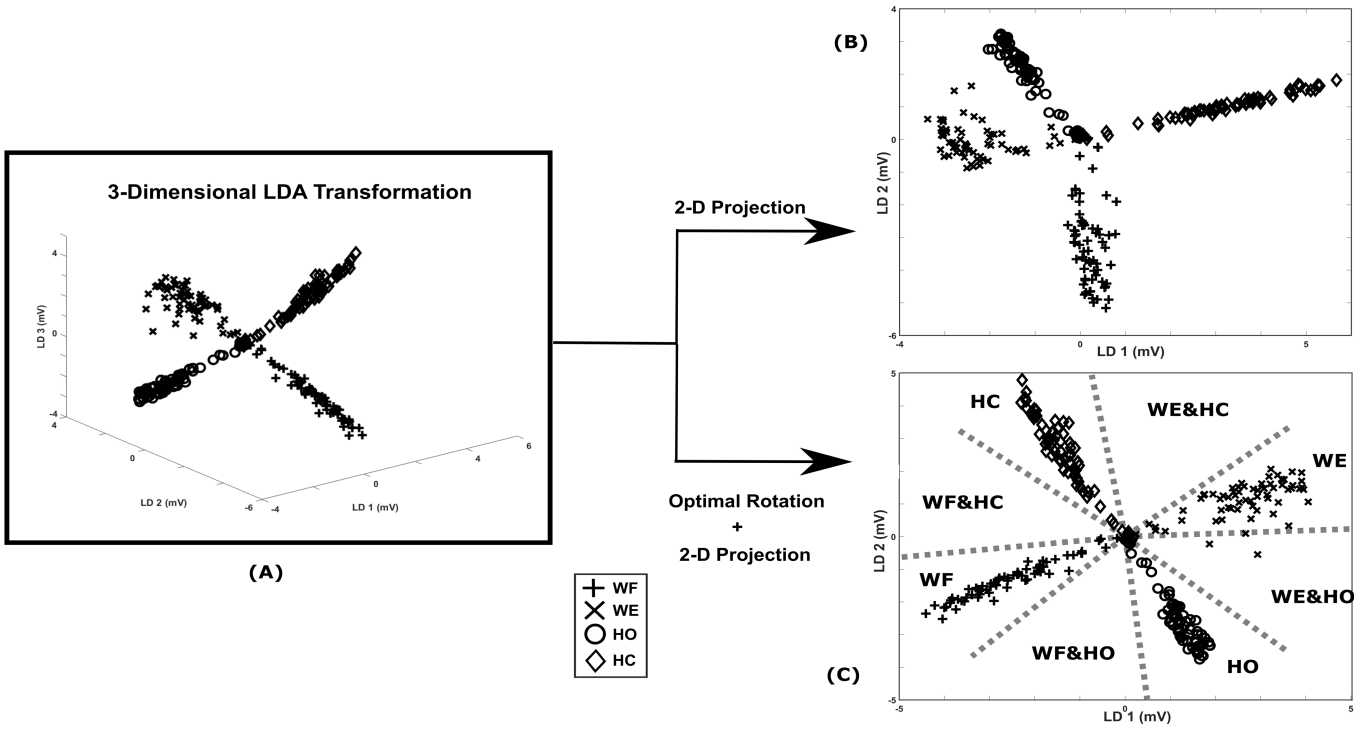

Fig. 5. A) The plot represents the three-dimensional LDA transformed EMG data of the 4 individual movements. B) The two-dimensional projection is represented in this plot, and it fails to meet the *orientation constraint* criteria, thereby invalidating the proposed decoding model. C) The transformed data after the optimal rotation and followed by two-dimensional projection is represented in this plot. It can be noticed that validity of the *orientation constraint* criteria is ensured, and the dotted lines indicate the boundaries for discriminating the various movements.

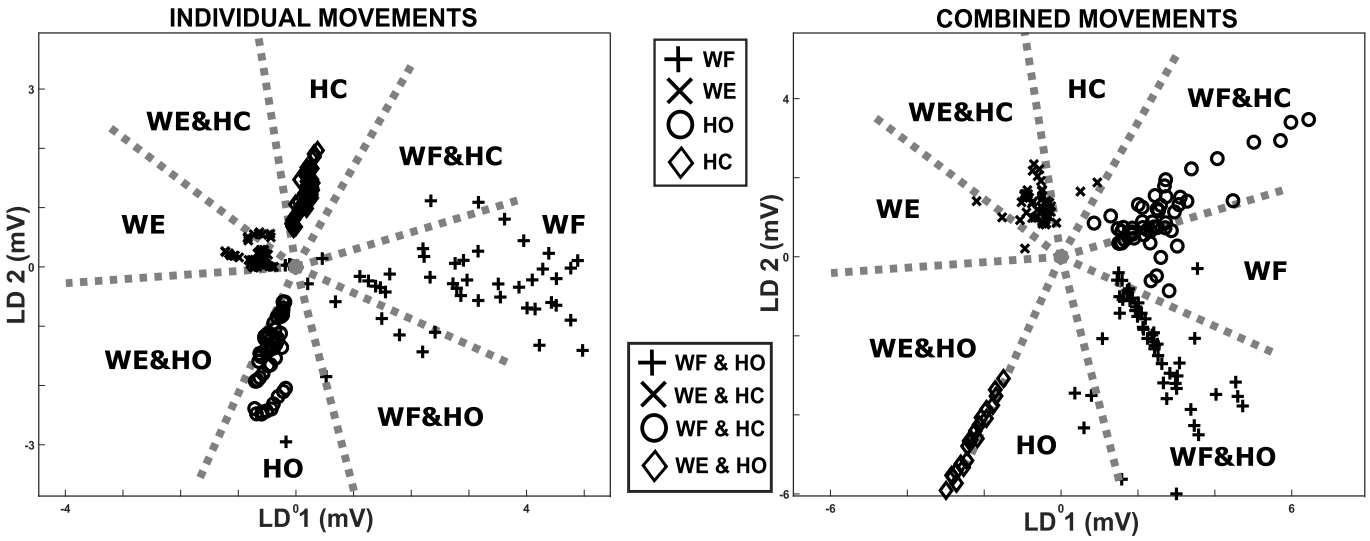

Fig. 6. The two-dimensional projection of the EMG data of a representative subject during the *online testing phase* is indicated. The plot on the left represents the data for the twenty trials for each of the individual movements, while the plot on the right correspond to the data of the combined movement trials.

The comparison of the accuracy with and without IDE is shown for each subject in Figure 7, where the individual motion data obtained during the *online testing phase* is used to evaluate the efficacy. The rate of misclassification of an individual movement as combined movement is shown to decrease for most of the subjects, and in such cases the prediction accuracy for individual motions have respectively improved. A one-way repeated anova test was performed to evaluate the significance in the differences between the misclassification rate. We observed a high significant difference ($p = 0.002$) with an F-ratio of 15.815.

A. Motion Selection Time

The average time taken to correctly select the desired motion class, across all subjects and motion classes is 0.52 ± 1.07 seconds. The mean selection time is higher in the case of simultaneous motions (0.78 ± 1.20) when

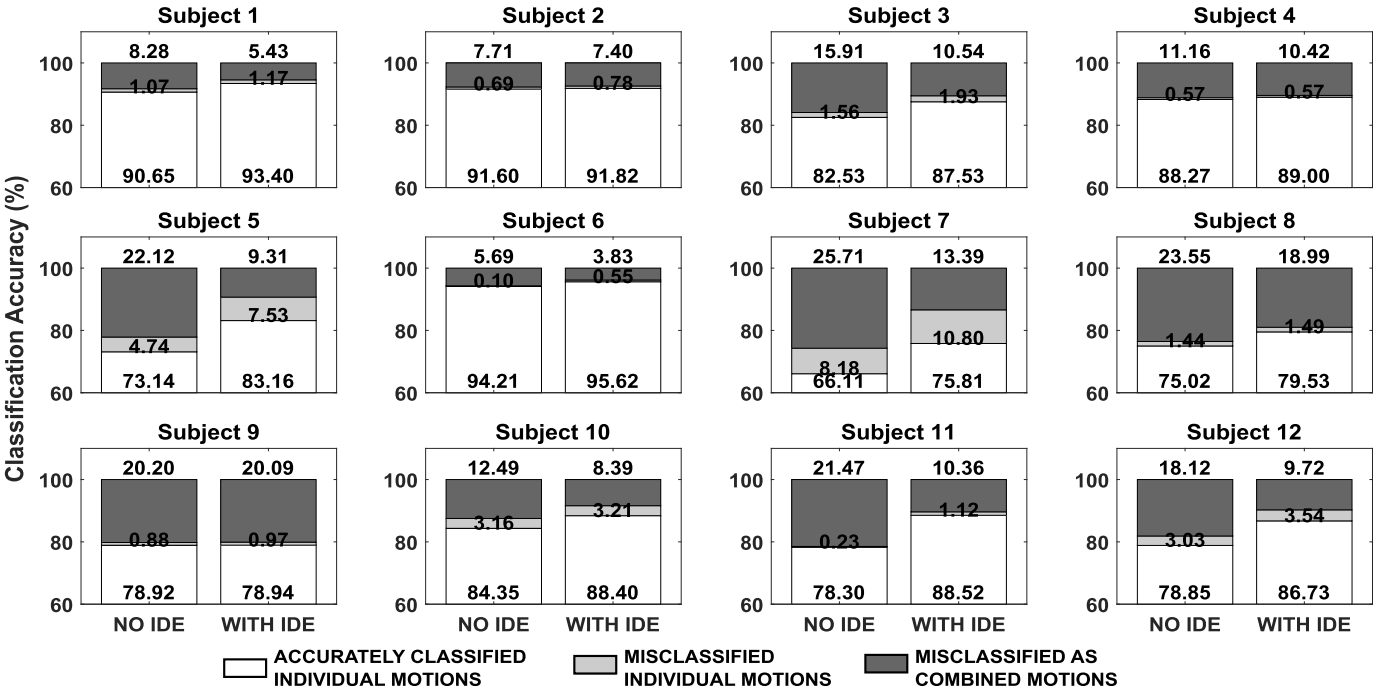

Fig. 7. Bar plots indicating the accuracy of decoding of the individual movements, and the misclassification rate for all the subjects. A comparison of the accuracies with and without the IDE technique is shown to highlight its importance.

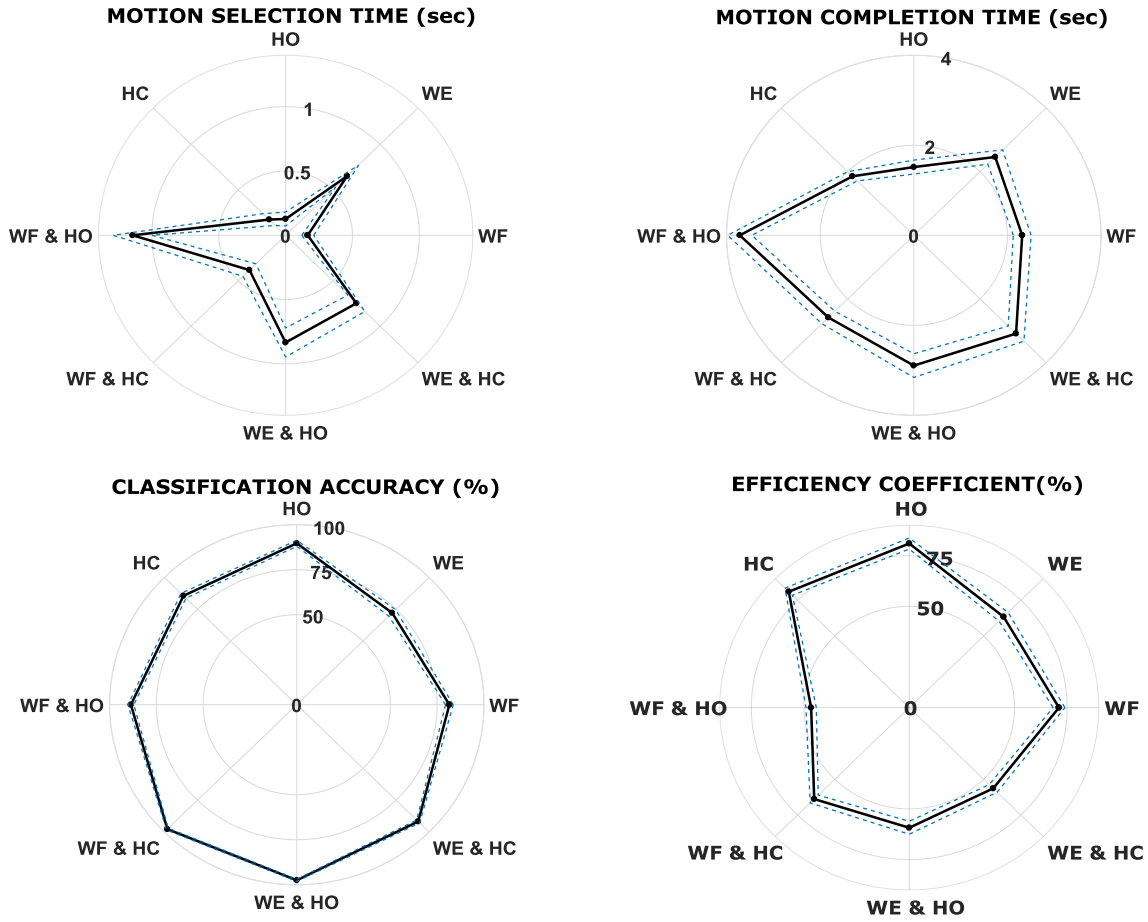

Fig. 8. Polar plot for the various performance metrics. Black lines and the dotted lines indicate the mean and standard error respectively in each motion-class across all subjects.

compared to individual motions (0.28 ± 0.87). A significant difference between individual and combined data-sets was found.

B. Motion Completion Time

The average time taken to complete each task across all the subjects and motion class is 2.53 ± 2.41 seconds. A statistical

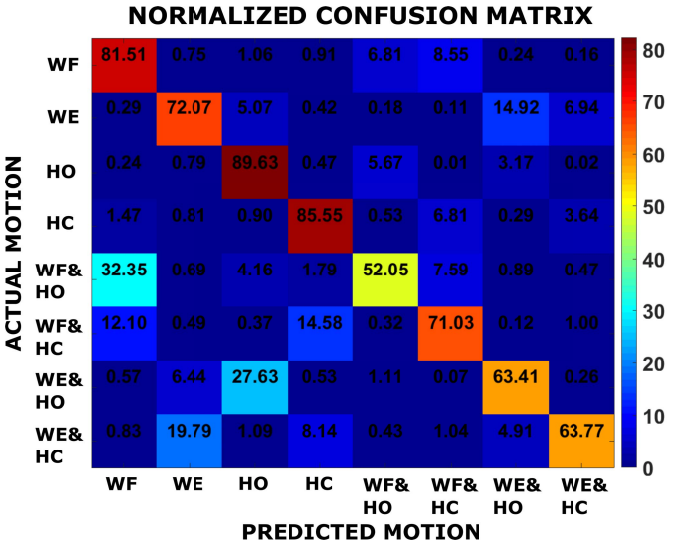

Fig. 9. Plot shows the confusion matrix of the classification accuracy concerning all the motion tasks.

significance is observed in the average values between individual (2.04 ± 2.02) and combined motions (3.06 ± 2.66), with the average time higher in the case of combined movements.

C. Online Classification Accuracy

The average classification performance of the decoder for all the subjects and across all the motion classes is $87.86 \pm 19.79\%$. There is also a statistical difference in the classification accuracy between individual ($82.1 \pm 23.56\%$) and combined motions ($93.94 \pm 12.15\%$), with combined movements having higher classification accuracy.

D. Efficiency Coefficient

The average efficiency coefficient of the decoder for all the subjects and across all the motion classes is $65.54 \pm 32.31\%$. There is also a statistical difference in the efficiency values between individual ($74.0 \pm 31.2\%$) and combined motions (56.64 ± 31.06), with combined movements having lower values in general.

Figure 8 represents the polar plot indicating the mean and standard error in the case of each of the movement classes across all subjects, for each of the performance measures.

The confusion matrix shown in Figure 9 reports the inaccuracy of the decoding model in predicting the user intention. We can notice that the accuracy of decoding the combined movements simultaneously, is low compared to that of the individual movements. This only means that an intended combined motion was performed sequentially, meaning that user starts with one individual motion-class followed by simultaneously performing the other respective class at some point in time to successfully complete the task. According to previous studies, unintended simultaneous motions were more detrimental to the control than unintended sequential motions [24]. The reason for a sequential approach could either be because of the higher threshold set in the MD algorithm to differentiate between individual and combined movements, or because the user intentionally preferred a sequential approach to complete the combined motion task. However, we observed a gradual change, from a sequential decoding to a more simultaneous decoding strategy, by the subjects as the trials progressed. In order to verify the learning trend, we measured the gradient of the line fitting the efficiency coefficient values during the twenty repetitions in the case of combined movements for each of the twelve subjects. A positive gradient value would suggest that the subjects progressively learn to simultaneously coordinate the movements, to efficiently reach the target during the online testing. Table I indicates the gradient values for each of the subjects and for the four combined motions; positive values were obtained for majority of the motions, indicating the presence of a learning effect. We did not perform a familiarization phase because our work does not contemplate any task which includes remapping of motor commands, kinematics or haptics, but rather the subjects were requested to replicate a motion task presented on a screen by a virtual avatar.

TABLE I
LEARNING RATES (GRADIENT VALUES) IN THE CASE OF THE FOUR COMBINED MOTIONS FOR ALL THE SUBJECTS

Subject	Wrist Flexion & Hand Open	Wrist Flexion & Hand Close	Wrist Extension & Hand Open	Wrist Extension & Hand Close
Subject 1	2.57	1.23	-0.26	2.10
Subject 2	-0.32	-0.33	0.76	-0.34
Subject 3	0.01	0.19	-0.29	-0.17
Subject 4	3.05	-1.02	-0.12	-0.62
Subject 5	-0.02	1.21	-0.08	-6.09
Subject 6	1.63	0.65	1.76	1.21
Subject 7	2.35	-1.38	-2.46	2.51
Subject 8	0.79	0.01	-0.56	0.67
Subject 9	0.98	0.96	-0.25	3.41
Subject 10	1.38	-0.81	0.84	1.32
Subject 11	0.32	-0.06	0.27	0.11
Subject 12	0.21	0.03	1.14	1.17

IV. DISCUSSION

The online testing of the proposed decoding strategy indicates good classification accuracy for both individual and combined motions involving the hand and wrist DOFs. Low-dimensional representation using the LDA plus optimal rotation transformation algorithm provides the basis for discriminating between individual and combined movements in a two-dimensional representation. We believe, that our approach is novel, and incorporates the strength of the LDA technique to build an algorithm capable of decoding both individual and simultaneous movements. As previously mentioned, the method proposed by Jiang *et al.* [16] for simultaneous motion decoding uses an NMF algorithm (unsupervised) to perform dimensionality reduction; one drawback of their approach is the need to determine a correction factor after the calibration in order to account for any potential reversal of direction due to the indeterminacy of the NMF algorithm. Our proposed decoding model does not have any directional indeterminacy due to fact that LDA is a supervised algorithm where both the agonist and antagonistic movements in a DOF are labeled. However, it is one of the first algorithms to

TABLE II
EFFICIENCY COEFFICIENT COMPARISON

NMF approach by Jiang et al. [16]		Our proposed LDA approach			
Sub	Efficiency Coefficient	Sub	Efficiency Coefficient	Sub	Efficiency Coefficient
H2	66.87±24.36	S1	74.14±10.28	S7	52.57±19.53
H5	64.01±22.74	S2	60.73±22.90	S8	60.37±24.03
H7	48.76±23.30	S3	59.72±26.23	S9	61.71±24.48
AG3	48.21±18.95	S4	63.16±24.56	S10	56.83±25.57
-	-	S5	57.88±21.97	S11	81.18±19.77
-	-	S6	68.70±25.37	S12	68.93±27.25

develop a strategy for decoding both individual and combined motions, by recording data from the singular movement, which is aligned with our proposed decoding strategy. While a comparison between the two approaches in terms of accuracy of decoding is not possible at the moment, due to the fact our proposed decoding strategy is built to perform discrete classification of movements rather than a proportional regression-based approach by the other group. However, we have added a table (Table II) to make a generic comparison of the efficiency coefficient metric in both the cases.

We notice better efficiency values while using our LDA based approach ($mean = 63.83\%$) compared to NMF based approach ($mean = 56.96\%$) by Jiang *et al.* [16], where both strategies use a position control model for the movement of the avatar or cursor. Though, the nature of the tasks is different in both the cases, this comparison is only meant to provide a coarse evaluation of our approach when compared to others. However, our next step will be in extending the usage of the decoding strategy to include proportional control, and hence an evaluation of the performance differences would be more appropriate. On the other hand, the approach by Young *et al.* is based on a strategy that involves recording data from both simple and multiple motions. However, the main aim of this study is primarily to introduce and evaluate the efficacy of a novel low-dimensional and computationally efficient decoding strategy capable of simultaneous decoding, by recording only the individual motions.

We notice that the efficiency coefficient values are higher in the case of individual motions when compared to combined motions. This reiterates the effectiveness of the IDE technique, in ensuring unintentional prediction of a combined motion when the user is intending to perform an individual motion. Though, the efficiency is lower in the case of combined motions, we do notice a gradual improvement towards an efficient way of performing the task, as characterized by the learning rates in the results section. Therefore, there is scope for an efficient way of performing both the types of motions using our approach.

Another aspect of our proposed decoding strategy is the potential to incorporate a modular approach, whereby scalability in terms of the number of DOFs can be achieved without increasing the complexity. This means that any n-DOF task ($n > 2$) could be split into smaller two-DOF task modules, and the outputs are then combined to perform simultaneous decoding. With a 'divide and conquer' strategy, along with the IDE technique to distinguish between individual and combined movements, our algorithm could potentially aid in increasing the number of DOFs, and this critical challenge will be an important focus for future works. Together with low-dimensionality of control and reduced computational cost, our aim is to implement the control algorithm in an embedded computing platform, to enable portability of the processing unit and perform faster real-time control in applications such as myoelectric-based prosthesis or exoskeletons.

One limitation of our proposed decoding strategy to be considered for future experiments is the lack of proportional control in movement position. However, the algorithm could be extended to incorporate proportional myoelectric control by evaluating the magnitude of the feature vector in the 2-dimensional plane after the modified-LDA transformation. The amplitude of the feature vector provides an estimation of the effort exerted by the user, and normalization procedures can be performed to ensure similar peak velocities across all classes. An optimization algorithm could be built to further reduce the calibration time especially for calculating the optimum rotation matrix. A cost function could be used to implement a gradient descent-based approach to arrive at the optimum Euler-angle values, instead on calculating the cost for all possible combinations of Euler-angles.

V. CONCLUSION

In this paper we presented a novel classification algorithm capable of decoding both individual and combined movements using a low-dimensional representation of the EMG signals using LDA transformation. The performance of the decoder was tested in the case of a two DOF motion task involving hand and wrist movements. The results indicate good decoding accuracy for both individual and combined motions. Incorporating an IDE technique based on MD measure has helped improve the decoding accuracy and prevent inadvertent activation of combined motions when individual motion is intended. Extending the control to incorporate proportional control as well as the capability to decode more than two DOFs would be implemented in future experiments. The current experimental setup consists of instrumentation which is not realized for portability and is tested in a virtual environment; the future goal would be to realize an embedded architecture to control either a prosthesis or a wearable exoskeleton device.

REFERENCES

[1] E. Chiovetto *et al.*, "Assessment of human-likeness and naturalness of interceptive arm reaching movement accomplished by a humanoid robot," *IEEE Trans. Robot.*, vol. 27, no. 5, pp. 943–957, 2011.
[2] C. Cipriani, F. Zaccone, S. Micera, and M. C. Carrozza, "On the shared control of an EMG-controlled prosthetic hand: Analysis of user–prosthesis interaction," *IEEE Trans. Robot.*, vol. 24, no. 1, pp. 170–184, Feb. 2008.
[3] S. A. Dalley, H. A. Varol, and M. Goldfarb, "A method for the control of multigrasp myoelectric prosthetic hands," *IEEE Trans. Neural Syst. Rehabil. Eng.*, vol. 20, no. 1, pp. 58–67, Jan. 2012.
[4] H. O. Kendall, F. P. Kendall, and G. E. Wadsworth, "Muscles, testing and function," *Amer. J. Phys. Med. Rehabil.*, vol. 52, no. 1, p. 43, 1973.
[5] M. Connan, E. R. Ramírez, B. Vodermayer, and C. Castellini, "Assessment of a wearable force- and electromyography device and comparison of the related signals for myocontrol," *Frontiers Neurorobot.*, vol. 10, p. 17, Nov. 2016.
[6] C. Castellini *et al.*, "Proceedings of the first workshop on peripheral machine interfaces: Going beyond traditional surface electromyography," *Frontiers Neurorobot.*, vol. 8, p. 22, Aug. 2014.

[7] K. Englehart, B. Hudgins, and P. A. Parker, "A wavelet-based continuous classification scheme for multifunction myoelectric control," *IEEE Trans. Biomed. Eng.*, vol. 48, no. 3, pp. 302–311, Mar. 2001.

[8] A. B. Ajiboye and R. F. Weir, "A heuristic fuzzy logic approach to EMG pattern recognition for multifunctional prosthesis control," *IEEE Trans. Neural Syst. Rehabil. Eng.*, vol. 13, no. 3, pp. 280–291, Sep. 2005.

[9] J. J. Baker, E. Scheme, K. Englehart, D. T. Hutchinson, and B. Greger, "Continuous detection and decoding of dexterous finger flexions with implantable myoelectric sensors," *IEEE Trans. Neural Syst. Rehabil. Eng.*, vol. 18, no. 4, pp. 424–432, Aug. 2010.

[10] A. J. Young, L. H. Smith, E. J. Rouse, and L. J. Hargrove, "A comparison of the real-time controllability of pattern recognition to conventional myoelectric control for discrete and simultaneous movements," *J. Neuroeng. Rehabil.*, vol. 11, no. 1, p. 5, 2014.

[11] J. L. Nielsen, S. Holmgaard, N. Jiang, K. B. Englehart, D. Farina, and P. A. Parker, "Simultaneous and proportional force estimation for multifunction myoelectric prostheses using mirrored bilateral training," *IEEE Trans. Biomed. Eng.*, vol. 58, no. 3, pp. 681–688, Mar. 2011.

[12] E. N. Kamavuako, D. Farina, K. Yoshida, and W. Jensen, "Estimation of grasping force from features of intramuscular EMG signals with mirrored bilateral training," *Ann. Biomed. Eng.*, vol. 40, no. 3, pp. 648–656, 2012.

[13] S. Muceli and D. Farina, "Simultaneous and proportional estimation of hand kinematics from EMG during mirrored movements at multiple degrees-of-freedom," *IEEE Trans. Neural Syst. Rehabil. Eng.*, vol. 20, no. 3, pp. 371–378, May 2012.

[14] N. Jiang, J. L. Vest-Nielsen, S. Muceli, and D. Farina, "EMG-based simultaneous and proportional estimation of wrist/hand kinematics in uni-lateral trans-radial amputees," *J. NeuroEng. Rehabil.*, vol. 9, no. 1, p. 42, 2012.

[15] L. H. Smith, T. A. Kuiken, and L. J. Hargrove, "Real-time simultaneous and proportional myoelectric control using intramuscular EMG," *J. Neural Eng.*, vol. 11, no. 6, Dec. 2014, Art. no. 066013.

[16] N. Jiang, H. Rehbaum, I. Vujaklija, B. Graimann, and D. Farina, "Intuitive, online, simultaneous, and proportional myoelectric control over two degrees-of-freedom in upper limb amputees," *IEEE Trans. Neural Syst. Rehabil. Eng.*, vol. 22, no. 3, pp. 501–510, May 2014.

[17] A. Ameri, E. N. Kamavuako, E. J. Scheme, K. B. Englehart, and P. A. Parker, "Support vector regression for improved real-time, simultaneous myoelectric control," *IEEE Trans. Neural Syst. Rehabil. Eng.*, vol. 22, no. 6, pp. 1198–1209, Nov. 2014.

[18] J. M. Hahne *et al.*, "Linear and nonlinear regression techniques for simultaneous and proportional myoelectric control," *IEEE Trans. Neural Syst. Rehabil. Eng.*, vol. 22, no. 2, pp. 269–279, Mar. 2014.

[19] L. H. Smith, T. A. Kuiken, and L. J. Hargrove, "Evaluation of linear regression simultaneous myoelectric control using intramuscular EMG," *IEEE Trans. Biomed. Eng.*, vol. 63, no. 4, pp. 737–746, Apr. 2016.

[20] M. Nowak, B. Aretz, and C. Castellini, "Wrist and grasp myocontrol: Online validation in a goal-reaching task," in *Proc. 25th IEEE Int. Symp. Robot Hum. Interact. Commun. (RO-MAN)*, Aug. 2016, pp. 132–137.

[21] C. Castellini and M. Nowak, "EMG-based prediction of multi-DOF activations using single-DOF training: A preliminary result," in *Proc. MEC-Myoelectr. Control Symp.*, 2014, pp. 45–49.

[22] M. Welling, "Fisher linear discriminant analysis," Dept. Comput. Sci., Univ. Toronto, Toronto, ON, Canada, Tech. Rep., 2005, vol. 3, no. 1.

[23] T. Flash and N. Hogan, "The coordination of arm movements: An experimentally confirmed mathematical model," *J. Neurosci.*, vol. 5, no. 7, pp. 1688–1703, 1985.

[24] S. Amsuess *et al.*, "Context-dependent upper limb prosthesis control for natural and robust use," *IEEE Trans. Neural Syst. Rehabil. Eng.*, vol. 24, no. 7, pp. 744–753, Jul. 2016.

[25] G. Li, A. E. Schultz, and T. A. Kuiken, "Quantifying pattern recognition—Based myoelectric control of multifunctional transradial prostheses," *IEEE Trans. Neural Syst. Rehabil. Eng.*, vol. 18, no. 2, pp. 185–192, Apr. 2010.